MMTO Conversion Technical Memorandum #00-3

Smithsonian Institution &
The University of Arizona®

6.5m MMT f/9-f/15 Hexapod Laboratory Calibration

S. C. West, D. Fisher, P. Spencer,

T. Trebisky, B. Hille, G. Weir

March 7, 2000

6.5m MMT f/9-f/15 Hexapod Laboratory Calibration

MMT Conversion Technical Memo #00-3, 07 Mar 2000

S.C. West, D. Fisher, P. Spencer, T. Trebisky
Multiple Mirror Telescope Observatory, Tucson, AZ
and
B. Hille and G. Weir
Steward Observatory Mirror Lab, Tucson, AZ

Abstract

We report the (Sept.-Oct. 99) laboratory certification of the 6.5m MMT shared hexapod positioning system for the f/9 and f/15 secondaries. A description of the testing apparatus is given. A summary of the inverse kinematic and vector force-torque modeling is presented. We measure positioning kinematics, stiffness, hysteresis, and repeatability under a variety of conditions.

I. Intro

ADS International s.r.l. was contracted to design and manufacture the hexapod positioner shared by the MMT f/9 and f/15 secondaries. This contract included testing/certification of individual strut actuators. Information concerning the design specifications, engineering analysis, and testing of the individual hexapod struts has been published[1][2].

Prior to installing the hexapod in the telescope, we subjected the assembled system to a range of tests including:

- verification of inverse kinematic positioning model and its elevation dependence.
- full load qualification and estimation of elevation-dependent strut forces.
- hysteresis/repeatability and its elevation dependence for both large and small strut length changes.
- compression to/from tension stiffness performance
- verification of a repeatable system reference or home position.

The description and results of these tests are reported in this memo.

II. Calibration fixture

A. Mechanical

A testing platform -- large enough to accommodate the f/5 secondary and its hexapod -- was designed and constructed at the Steward Mirror Lab for the MMTO (Figure 1). The box frame is attached to the base with a trunnion. The frame can be moved to adjust the cg of the load onto the trunnion axis. A hand crank allows the selection of the elevation for testing.

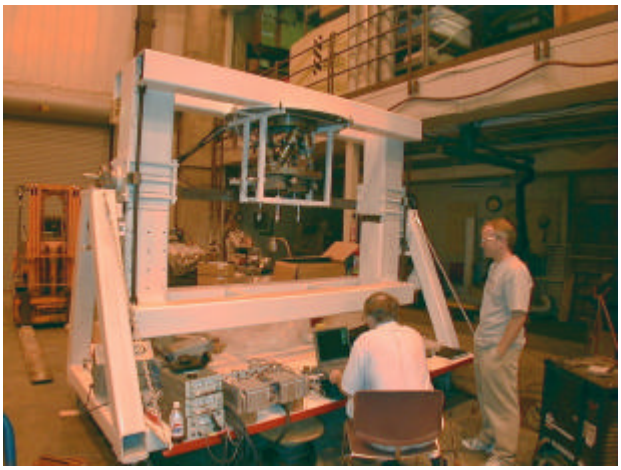

Figure 1: Calibration fixture manufactured for testing the hexapod and secondary mirror systems. It is shown here with the f/9 hexapod attached. The fixture is large enough to fully test the f/5 secondary and its positioning system when it is finished. Shown here are Pete Spencer (right) and Don Fisher of the MMTO.

The f/9 hexapod is attached to the box frame (Figure 2) and placed under its designed load of 160 kg with two steel plates and a granite research-grade master tri-square.

B. Electronics

The motion of the tri-square -- produced by changes in the hexapod strut lengths -- is determined by reading six lvdts in contact with three of the granite surfaces. We chose Sensotec BY132HQ DC-DC lvdts with a two-inch stroke. A computer controlled data acquisition unit (HP 34970A DAU with an HP

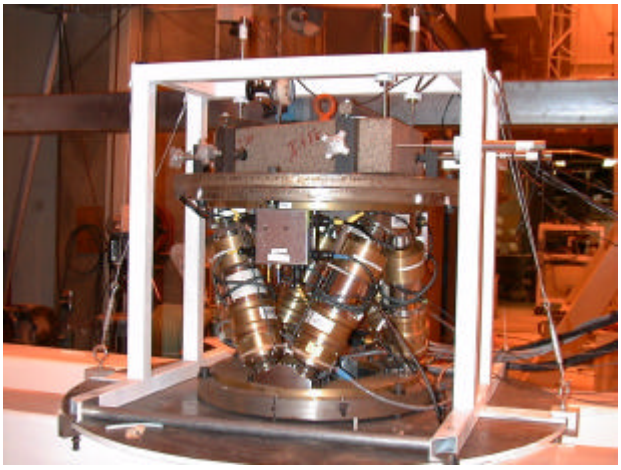

Figure 2: Closeup of the hexapod attached to the test fixture. Part of the load is a Starett granite master tri-square contacted by six LVDTs so that the computer can resolve the motion of the hexapod mobile platform vs. changes in strut length.

34901A mux) was used to read the voltages output by the LVDTs. This instrument was operated using a 10 volt signal with 5.5 digits of precision. The HP 34970's analog to digital converter operated synchronously with the 60 Hz line power to eliminate pickup. 100 readings were averaged at each position to improve the SNR. Noise in the system (measured with no power to the LVDTs) was measured to be less than one count in our least significant digit.

C. Software

An interactive TCL/TK interface GUI was written to control all of the hexapod functions. The calibration setup contained two sets of six LVDTs. One set provided an LVDT coaxial with each actuator. The other set was attached directly to the granite tri-square, as shown in Figure 2. The positioning matrix (eq 1 in section IIIA) and its inverse were incorporated into the control interface. These matrices allowed commands in either coordinate system to be input (*i.e.* actuator lengths or mobile plate position). The two independent sets of LVDT data -- along with positions returned by the servo system -- provided convenient cross checks and error determinations.

The code for this experimental setup was implemented in Octave. Octave was chosen because it is a mathematical interpretive language allowing real time control of data acquisition and analysis. To support data acquisition, routines were added to octave to control the HP 34970A DAU. The computer communicates with the DAU using ascii control strings transmitted over an RS232 interface. Instrument status and data are acquired over the same interface.

Codes written in Octave controlled which LVDTs were read, the amount of signal averaging etc. Octave was extended to provide a socket interface that allowed communication with the VxWorks control computer. This facility allowed the data acquisition code to both move the platform and acquire the data.

III. Models

The calibration process is facilitated by producing position and force models of the hexapod so that the behavior of the platform can be estimated *a-priori*.

A. Inverse kinematic solution

The process of solving for the length changes of the adjustable struts from a given change in the mobile plate position is termed the inverse kinematic solution. It is a relatively straightforward geometric exercise. The attachment coordinates are used to make a vector for each strut. The 6 attachments to the mobile plate are translated and rotated via an Euler matrix and a decenter vector. Redrawing the vectors gives the length changes of the struts for the desired motion. Strut length sensitivities to each degree of freedom of the mobile plate are combined to give a matrix that predicts the total strut length change for any desired motions of the mobile plate. Because the movement volume of this hexapod is very small, all the matrix terms are linear, and this method works well.

The change in strut lengths (Δli) are related to the motion of the mobile platform by:

$$\begin{bmatrix} -374.9 & -191.5 & 907.1 & 0.383 & 0.852 & 0.492 \\ 374.7 & -191.5 & 907.1 & -0.383 & -0.852 & 0.492 \\ 21.49 & 420.2 & 907.1 & 0.383 & -0.852 & 0.492 \\ -21.76 & 420.2 & 907.1 & -0.383 & 0.852 & 0.492 \\ 353 & -229 & 907.1 & 0.383 & -0.0002 & -0.9841 \\ -353.3 & -229 & 907.1 & -0.383 & -0.0002 & -0.9841 \end{bmatrix} \begin{bmatrix} \Delta x \\ \Delta y \\ \Delta z \\ \Delta\theta z \\ \Delta\theta y \\ \Delta\theta x \end{bmatrix} = \begin{bmatrix} \Delta l0 \\ \Delta l1 \\ \Delta l2 \\ \Delta l3 \\ \Delta l4 \\ \Delta l5 \end{bmatrix} \quad (1)$$

where the first three columns have units of $\mu m/\mathrm{mm}$, and the last three have $\mu m/\mathrm{arcsec}$. Given the mobile platform x,y,z translations (mm) and tilts (arcsec), the strut length change in microns can be found. The angles are resolved about the vertex location of the f/9 secondary in its telescope cell.

The details of this model can be found at http://nemo.as.arizona.edu/~swest/f9hex_calib/f9strutLength.pdf and are derived from the analysis used for the primary mirror hardpoint platform [3] and the calibration of the VATT secondary linkage[4].

B. Strut forces vs. elevation

A vector model was used to calculate the forces applied to the struts due to load and gravity vector. Forces and moments applied to the mobile plate (about the cg of the load) are resolved into strut forces using the 3-D torque equation. The analysis is shown at http://nemo.as.arizona.edu/~swest/f9hex_calib/f9forces.pdf and is derived from the work done with the primary mirror hardpoint platform[5].

The results of the strut load modeling vs. elevation are shown in Figure 3 for a load of 160kg about the cg plane of the f/9 secondary system.

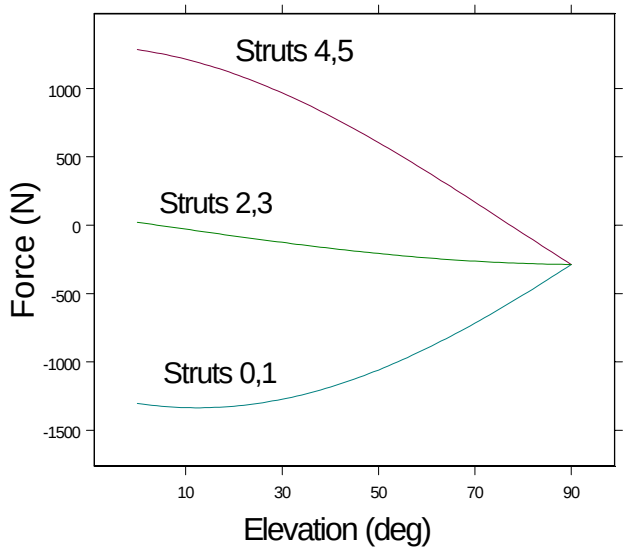

Figure 3: Estimate of the force (N) vs. elevation angle (deg) for the three strut pairs determined from the vector model of the hexapod.

IV. Tests/Calibrations

A. Inverse kinematic verification

The positioning behavior predicted from the inverse kinematic model was verified with the calibration fixture. As Figure 2 shows, six lvdts contact the research-grade granite tri-square. Each lvdt is sensitive to motion along one axis of the system. By knowing the contact point of each lvdt on the tri-square relative to the vertex position of the secondary mirror -- and the axis to which it's sensitive -- the rigid-body motion of the tri-square due to strut length changes is calculated from the six lvdt displacements. The details of these calculations (and for all the results found here in section IV) are found in http://nemo.as.arizona.edu/~swest/f9hex_calib/f9calib.mcd.pdf.

The positioning matrix given in Section IIIA was verified using this technique. It was expected that the matrix terms would be refined slightly due to the geometry of the vane flexures and any deviation of the as-built hexapod to the conceptual design. However, the accuracy with which we could determine the position of the tri-square attached to the mobile plate limited any significant refinement of the terms.

We verified the decenter matrix elements to about 0.03% (limited by the measurement accuracy of the lvdts) and the tilt terms to about 0.5% (limited by the uncertainty in the absolute position of the center of the tri-square from the hexapod axis). This verification was done at three orientations: the equivalent of telescope zenith pointing (actuators in tension), nadir pointing (compression), and horizon pointing (mixed tension and compression). As expected, the positioning matrix terms and performance had no elevation dependence.

Data were also taken measuring the influence of each strut on the rigid-body motion of the mobile platform (direct kinematic measurement). These data could be used to produce a positioning matrix equivalent to Equation 1, but given the successful verification of the vector model for a few test cases, these data were simply archived.

B. Hysteresis and repeatability

While keeping the gravity orientation of the hexapod fixed, the position of the mobile plate was cycled. For these tests, all actuators were given the same position commands so that the mobile plate was moved in pure z-motion. The motion of the mobile platform was measured by averaging the 3 lvdts contacting the tri-square along the z-direction. This test is sensitive mainly to roller screw hysteresis, play in the bearings that support the drive shafts, and systematics in our measurement system.

Figure 4 shows the fine-motion hysteresis/repeatability that we observed. The non-repeatability is $\pm 1.5\ \mu m$ except at

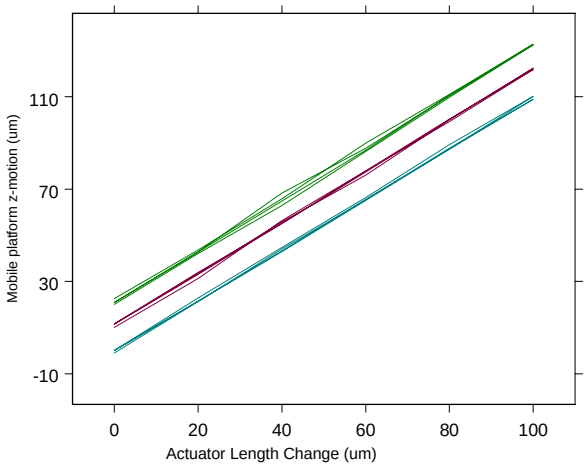

Figure 4: Hysteresis for small changes in actuator length for: zenith pointing (lower, actuators in tension), nadir pointing (middle, actuators in compression), and horizon pointing (upper, mixed compression and tension). In each position, all the actuators were moved in 20 micron increments for two full cycles of 100 microns amplitude. The averaged z-motion of the granite reference is plotted against the actuator length change. Each data set is plotted with a 10 micron y-offset for clarity.

horizon pointing where is expanded to $\pm 3\ \mu m$. The zenith-pointing telescope specification for the M1 to M2 spacing is $\pm 6\ \mu m$ [6].

The reversed-cycle hysteresis/repeatability over an 18mm range of the actuators was also measured. This was a severe test over a range far exceeding the operating parameters of the telescope (and hexapod), and the observed hysteresis/repeatability was < 0.07% of the full range.

C. System Stiffness

Average platform stiffness

The total stiffness of the hexapod was measured by reversing the 160 kg load from tension to compression while reading the length change of the struts and the displacement of the tri-square. Figure 5 shows the average displacement responses to

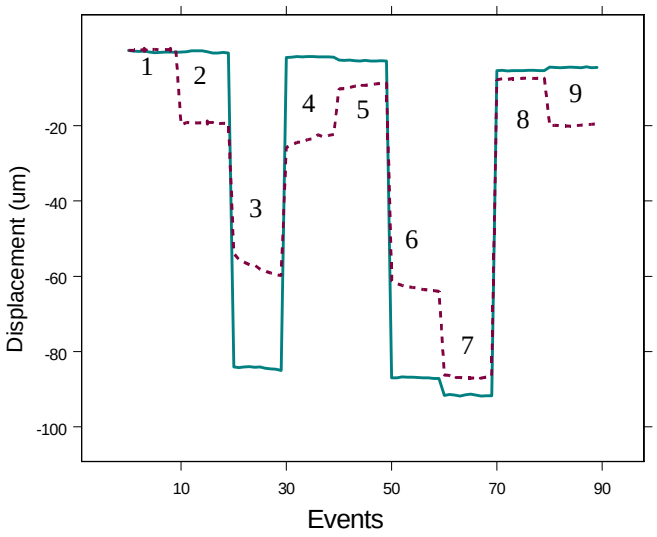

Figure 5: Averaged response of the tri-square sensors (solid) and the actuator sensors to 160kg of load switched from tension to compression with and without strong impulses applied to the testing fixture. See text for details.

9 events (the impulses consisted of hitting the box frame of the calibration fixture with a large 4x4 in order to remove any potential friction/stiction in the measurement systems):

- 1: load placing all actuators in compression.
- 2: compression after a heavy impulse to fixture.
- 3: Invert fixture to put actuators in tension.
- 4: rotate back to compression
- 5: compression after a heavy impulse
- 6: Invert back to tension
- 7: Tension after heavy impulse
- 8: Back to compression
- 9: Compression after heavy impulse

The agreement between the two data sets is quite good. Because of the strut geometry, $\Delta z = \Delta l/\cos(\theta_z)$ where θ_z is the angle between the strut and z axes (24.8 deg) and Δl is the change in strut length shown by the dotted line in Figure 5.

The reversed load of 160 kg corresponds to 3140 N which implies a total hexapod platform stiffness along the z-direction $k_z > 40\ N/\mu m$ (using the difference between regions 7 and 9 in Figure 5). The relationship between k_z and the strut stiffness k_s is $6k_s = k_z/\cos(\theta_z)^2$ giving an average strut stiffness of $\sim 8\ N/\mu m$ (using the granite lvdts) and $9\ N/\mu m$ (using the actuator lvdts). This is somewhat less than the $11\ N/\mu m$ measured by ADS [2]. However, this measurement includes any "slippage" in the actuator internals caused by moving from tension to/from compression (not included in the ADS analysis).

Individual strut stiffnesses

Figure 5 displays the average motion of the tri-square and actuators. The response of the individual actuators to the reversed load is shown in Figure 6. Actuators 2 and 5 show

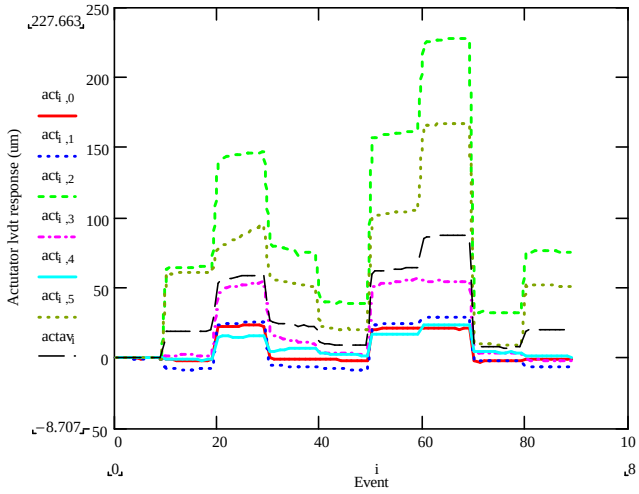

Figure 6: Response of the individual actuator lengths to the events shown in Figure 5.

significantly greater compliance than the others. The length changes due to an impulse suggest internal slippage of the screw shaft. In fact, the more compliant the actuator, the larger the length change created by the impulse -- lending more credence to some internal slippage dominating the stiffness of a few actuators. The stiffest actuators exceed $20\ N/\mu m$ and show no significant slippage response to impulses.

D. Position reference and brake cycling

Home position

The simplest method to establish a reference or home position for the hexapod is to use the lvdts mounted on the actuators themselves. It is important however to have an alternate

method in case the lvdts fail. Each actuator has limit switches at the travel extremes. The length of the actuator can be referenced to the point where the limit switches are just triggered. The incremental encoder generates an index pulse once per revolution. Additional accuracy can be obtained by sensing the index pulse after using the limit switch to reference an absolute screw revolution. Table 1 summarizes the measured accuracy of these alternate methods in establishing a reference position for the hexapod. The data were collected by repeatedly re-establishing the reference point and analyzing the final positions of the tri-square reference. Using limits by themselves without the index pulse repeats better than expected.

Table 1: Accuracy of alternate techniques to establish a position reference.

Reference Technique	standard deviation microns	p-v microns
limits alone	3.2	8.6
limits and index pulse	1.9	5.3

Brake cycling

Each actuator incorporates a disk brake that allows the position to be locked prior to de-energizing the motor between position updates. The precise position change of the tri-square was repeatedly measured as the brakes and motors were cycled. We could not detect any motion larger than the measurement noise in the tri-square measuring system (about $(\pm 0.2)\ \mu m$).

This confirms the results of brake testing done during the selection process for the actuator components. It was found that engaging the brake produced a $0.025\ \mu m$ change in linear position of a 1mm pitch screw[7].

V. Conclusions

The hexapod positioner that is shared between the MMT f/9 and f/15 secondaries was rigorously tested in the laboratory prior to installation at the telescope. The inverse kinematic positioning model was verified. Both large and small scale hysteresis and repeatability were found to meet our optical collimation specifications. The effective stiffness of the platform and struts were measured and they compared favorably to the single actuator measurements made by ADS. The average platform performance was not significantly degraded by varying gravity, and the actuators performed adequately in the tension to compression crossover regions.

VI. Data Files

- http://nemo.as.arizona.edu/~swest/f9hex_calib/f9hexcalib.pdf, ps: this document in pdf and ps formats.
- http://nemo.as.arizona.edu/~swest/f9hex_calib/f9strutLength.pdf: details of the inverse kinematic model.
- http://nemo.as.arizona.edu/~swest/f9hex_calib/f9forces.pdf: 3-D force-torque vector model.
- http://nemo.as.arizona.edu/~swest/f9hex_calib/f9calib.mcd.pdf: mathcad file showing reduction of all data obtained with the calibration fixture.

VII. Acknowledgments

Shawn Callahan and Court Wainwright of the MMTO helped with the installation and removal of the hexapod from the calibration fixture as well as other mechanical details. We had helpful discussions with Brian Cuerden and Scott DeRigne of the Steward Technical Division. John McAffee and Ken Vanhorn (MMTO) and Vince Moreno (SOTD) helped assemble and build much of the electronics.

VIII. References

[1] W. Gallieni and R. Pozzi, “Secondary Mirrors Support M2/F15 and M2/F9 Hexapod Design,” *Multiple Mirror Telescope Observatory Technical Report* **#31**, January 1997.

[2] D. Gallieni, “M2/f15 and M2/f9 Hexapod Data Package,” *Multiple Mirror Telescope Observatory Technical Report* **#34**, July 1998.

[3] S.C. West, “A Hardpoint Calculator for the MMT Conversion,” *MMT Conversion Tech. Memo* **#96-1**.

[4] S.C. West, et al. “Progress at the Vatican Advanced Technology Telescope,” Optical Telescopes of Today and Tomorrow, SPIE 2871, ed. Arne Arnenberg, Hven Sweden, 74-85, 1996.

[5] S.C West, “Hardpoint platform matrices for the MMT 6.5m primary mirror cell,” *MMT Conversion Internal Tech. Memo* **#97-2**.

[6] D. Fabricant, B. McLeod, and S.C. West, “Optical Specifications for the MMT Conversion,” *Multiple Mirror Telescope Observatory Technical Report* **#35**, December 21, 1999 (*see e.g.*, section 7.4).

[7] B. Cuerden and R. Teachout, “MMT f/9 Hexapod Brake Motion on Application Electroid EFSB-15 with anti-backlash option,” *Steward Observatory Technical Services Memo*, Nov. 13, 1996.